

Chapter 2

NMR spectroscopy

NMR spectroscopy is used within practically all branches of natural and material sciences to determine structures of small to medium-sized molecules and to study their physical properties, interactions and dynamics. In fact, NMR is to date the only technique available to determine biomolecular structures in solution at atomic resolution. The ever growing impact of NMR has been made possible by two major advances: the development of pulsed Fourier transform (FT) NMR (Ernst & Anderson, 1966) and the concept of multi-dimensional NMR spectroscopy (Jeener, 1971). Technical improvements such as superconducting magnets with yet stronger fields and enhanced computer performance to deal with time-domain spectra have further extended the applicability of NMR. Since homonuclear spectra suffer severely from spectral overlap as molecular weight increases, methods to produce isotopically (^{13}C and/or ^{15}N) enriched biomolecules and the successive development of heteronuclear multi-dimensional NMR experiments were further break-throughs in the field of biomolecular NMR. Most recently, the accessibility of distance-independent angular information to structure determination (Tolman *et al.*, 1995; Tjandra & Bax, 1997; Tjandra *et al.*, 1997a) as well as the development of relaxation optimised NMR experiments and deuterium labelling techniques to reduce the line-widths of larger molecules (Pervushin *et al.*, 1997) promise to further increase the impact of NMR in future.

2.1 Principles of NMR spectroscopy

As all spectroscopic methods, NMR relies on the ability of matter to interact with electromagnetic radiation. Thereby, energy quanta are absorbed and/or emitted as a result of discrete energy state transitions according to the Bohr frequency condition

$$\Delta E = h\nu, \tag{2.1}$$

where ΔE is the energy difference between the final and the initial state, h is Planck's constant and ν the frequency of electro-magnetic radiation. The phenomenon of magnetic resonance

arises from a quantum mechanical property called spin, which confers a spin angular momentum \hat{I} to some nuclei. Although there is no classical analogue to the spin angular momentum, its physical properties can be grasped by considering a whipping top. The spinning motion of the top is (apart from friction and gravitation) a result of the inertia of rotational motion known as conservation of angular momentum. Therefore, many concepts used in NMR can be derived from angular momentum theory.

As the nucleus spins, so does its charge. This results in a nuclear magnetic moment $\vec{\mu}$, which is directly proportional to the spin angular momentum

$$\vec{\mu} = \gamma\hbar\hat{I}, \quad (2.2)$$

where γ is a nucleus-specific proportionality constant termed the gyromagnetic ratio, while \hbar equals h divided by 2π . The angular momentum operator \hat{I} is associated with two interdependent spin quantum numbers: the nuclear spin I and the magnetic (or azimuthal) spin quantum number m_I , which determine the magnitude $\hat{I}^2 = I(I+1)$ and the z -component $I_z = m_I = I, I-1, \dots, -I+1, -I$ of the spin angular momentum, respectively.

Nuclei with odd mass numbers (*e.g.* ^1H , ^{13}C and ^{15}N) possess half-integer spin, *i.e.* $I = \frac{1}{2}$ and hence $m_I = \pm\frac{1}{2}$. Nuclei with even mass number, but an odd number of protons have integer spin ($I = 1$ and hence $m_I = 1, 0, -1$ for *e.g.* ^2H and ^{14}N). In contrast, nuclei with even numbers of protons and neutrons, such as ^{12}C and ^{16}O , have zero spin and are thus “NMR-inactive”. Since most nuclei present in biomolecules are spin- $\frac{1}{2}$ nuclei, the following discussion will be limited to nuclear magnetic dipoles.

2.1.1 Effect of a static magnetic field

NMR spectroscopy exploits the fact that the nuclear magnetic moment $\vec{\mu}$ can interact with an applied, external magnetic field. The energy of this interaction is given by

$$E = -\mu_z B_0 = -\gamma\hbar m_I B_0 \quad (2.3)$$

if the direction of the external static magnetic field is defined along the z -axis. In the presence of a static magnetic field, the degenerate $2I+1$ nuclear spin energy levels split up according to their magnetic quantum number m_I (Zeeman interaction). Consequently, there are two energy states for a spin- $\frac{1}{2}$ nucleus: a so-called α -state with energy $+\frac{1}{2}\gamma\hbar B_0$ (spin-up) and a β -spin state with energy $-\frac{1}{2}\gamma\hbar B_0$ (spin-down) (Fig. 2.1 (a)). The energy difference between the two spin states is hence proportional to the magnetic field strength and the gyromagnetic ratio. The latter can therefore be regarded as a measure for the sensitivity of a nucleus for NMR.

However, as the nucleus is spinning, the magnetic dipole does not align completely with the magnetic field, but experiences a torque giving rise to a rotational motion (precession)

about the direction of the magnetic field B_0 at Larmor frequency

$$\omega_0 = -\gamma B_0 = \frac{\Delta E}{\hbar}. \quad (2.4)$$

Since the energy of the α -state is lower than for the β -state, more spins orient parallel than anti-parallel to the static magnetic field. The nuclear magnetic moments present in an NMR sample hence sum up to a net magnetisation \vec{M} along the direction of the static magnetic field (longitudinal magnetisation). On the other hand \vec{M}_x and \vec{M}_y (transverse magnetisation) average out, as the individual spins precess randomly about B_0 (Fig. 2.1(b)).

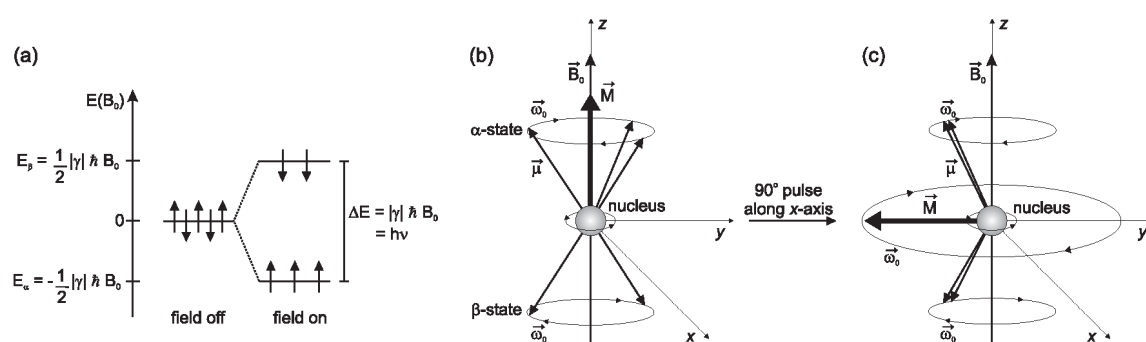


Figure 2.1: Magnetic moment of a spin-1/2 nucleus with negative gyromagnetic ratio. (a) Nuclear spin energy levels in the absence and presence of a static magnetic field B_0 . (b) Net magnetisation \vec{M} and orientation and precession of nuclear magnetic moments $\vec{\mu}$ in thermal equilibrium (longitudinal magnetisation). (c) Coherent precession of the magnetic moments after a 90° pulse applied along the x -axis giving rise to a rotation of \vec{M} in the x, y -plane (transverse magnetisation) at Larmor frequency ω_0 .

2.1.2 Radio frequency pulses

Due to the tiny nuclear spin population difference, energy state transitions can not be detected directly in an efficient manner, as is done in other spectroscopic methods. In addition, the nuclei in a molecule resonate at slightly different frequencies (section 2.1.3), and a range of frequencies must be excited to obtain a complete NMR spectrum. Thus the approach taken in NMR is to bring the system into a non-equilibrium state by a short radio-frequency (RF) pulse (Fourier transform or, briefly, FT NMR) (Ernst & Anderson, 1966). As a result, all spins precess with the same phase (coherence) and the magnetisation rotates with Larmor frequency in the x, y -plane (transverse magnetisation) (Fig. 2.1(c)) inducing a detectable current in the receiver coil. However, as spin synchrony is lost over time due to relaxation, the signal decays exponentially and is therefore referred to as free induction decay (FID). Since the detected signal is caused by nuclei precessing at slightly different Larmor frequencies, the FID is a superposition of all resonance frequencies as a function of time. Fourier transformation of the FID (processing) yields the spectrum in the frequency domain, which can be used for spectral

analysis.

Varying the length or the strength of the applied radio-frequency pulse, the magnetisation \vec{M} can be rotated by any desired angle (Fig. 2.1 (c)). For instance, a $180^\circ(\pi)$ -pulse inverts the populations of the nuclear spin states and thus the direction of the magnetisation.

2.1.3 Chemical shift

According to (2.4), all spins of the same nucleus type in a molecule should experience the same magnetic field and, hence, resonate at the same frequency, which would render NMR useless for structural investigations. Fortunately, the latter is not the case. The effective magnetic field experienced by a nucleus is modulated by the electronic structure around the nucleus. The source of this modulation is the motion of the surrounding electrons, which creates an additional, so-called secondary magnetic field shielding the external magnetic field. Therefore, slightly different resonance frequencies (chemical shifts) arise for nuclei that are not chemically equivalent

$$\nu_i = -\frac{\gamma B_0}{2\pi}(1 - \sigma_i), \quad (2.5)$$

where ν_i is the resonance frequency of a given nucleus i and σ_i its average shielding constant in isotropic solution. Since chemical shifts are very small (in the order of 10^{-6}) and according to (2.5) dependent on the magnetic field strength, they are measured in ppm (parts per million) relative to a reference frequency ν_{ref}

$$\delta_i^{\text{ppm}} = \frac{\nu_i - \nu_{\text{ref}}}{\nu_{\text{ref}}} \cdot 10^6 \approx (\sigma_{\text{ref}} - \sigma_i) \cdot 10^6. \quad (2.6)$$

Due to the sensitivity of the chemical shift to the local environment, functional groups of a molecule can often be directly identified based on their chemical shifts. Moreover, chemical shift changes are widely used to monitor conformational and electrostatic changes induced by ligand binding, pH or temperature variation. Using *e.g.* the deviation of protein backbone chemical shifts, in particular those of $^{13}\text{C}^\alpha$ atoms, from random coil chemical shifts (secondary chemical shifts) one can directly define secondary structure elements in proteins. In this Thesis, chemical shift changes upon ligand binding were used to map protein binding sites (Chapter 6 and 7).

2.1.4 Scalar and dipolar coupling

The magnetic dipoles in a sample can interact with each other directly (through-space) or indirectly *via* chemical bonds (through-bond). Magnetisation can hence be transferred from one involved spin to another by through-bond scalar couplings, which is the principle underlying J-correlated spectroscopy (COSY and related experiments) (Aue *et al.*, 1976; Braunschweiler

& Ernst, 1983), or by direct dipolar interactions giving rise to the so-called nuclear Overhauser effect (NOE). As the magnetisation transfer rate by direct dipolar coupling depends on the distance between the spins, the NOE yields important distance information that can be used for structure determination.

The indirect dipolar coupling interaction (scalar coupling or J -coupling) leads to the splitting of the resonance lines of two J -coupled nuclear dipoles in solution. The separation of the lines is given by the scalar coupling constant J . Since three-bond J -coupling constants (3J) depend on the torsion angles between the coupled spins, they yield important dihedral angle information for the structure calculation. This dependence is described by the semi-empirical Karplus equation (Karplus, 1963)

$${}^3J = A \cos^2 \phi + B \cos \phi + C, \quad (2.7)$$

where A , B and C depend on the types of coupled spins and ϕ is the torsion angle between the coupled spins.

2.2 Quantum description of NMR

While the behaviour of isolated nuclear spins during an NMR experiment can be described by classical vector models, coupled nuclear spin systems require a quantum mechanical treatment. Since NMR structure determination relies on experiments based on through-bond and through-space dipolar coupling interactions, the quantum mechanical concepts underlying the employed NMR experiments are discussed in the following.*

In quantum mechanics, the evolution of a system is governed by the time-dependent Schrödinger equation

$$\frac{d}{dt}|\Psi(t)\rangle = -i\hat{\mathcal{H}}(t)|\Psi(t)\rangle, \quad (2.8)$$

where $\hat{\mathcal{H}}$ is the Hamilton operator corresponding to the classical expression of the energy of a given interaction.† In a system of N spin- $\frac{1}{2}$ nuclei, each state vector $|\Psi\rangle$ can be written as a linear combination of the 2^N orthonormal eigenstates $|\psi_i\rangle$

$$|\Psi(t)\rangle = \sum_{i=1}^{2^N} c_i(t)|\psi_i\rangle = \sum_{i=1}^{2^N} c'_i \cdot e^{-i\phi t}|\psi_i\rangle, \quad (2.9)$$

where the time-dependence of the state vector is expressed by the complex coefficients $c_i(t)$, which include a phase factor $e^{-i\phi t}$. A physical observable in an independent quantum mechanical system is given by the expectation value of the corresponding operator defined as

*More detailed descriptions can be found in *e.g.* Abragam (1961); Ernst *et al.* (1987); Goldman (1988); van de Ven (1995); Cavanagh *et al.* (1996).

†Here and in the following, Hamiltonians are given in angular frequency units, *i.e.* $\hbar = 1$.

$\langle \hat{\mathcal{A}} \rangle = \langle \Psi | \hat{\mathcal{A}} | \Psi \rangle$. However, in NMR one deals with a large ensemble of spin systems, which interact with each other and the environment and hence exhibit a distribution of eigenstates and expectation values. To simplify the quantum mechanical description one considers in such cases only the ensemble-averaged expectation value

$$\overline{\langle \hat{\mathcal{A}} \rangle} = \sum_k \mathcal{P}_k(\Psi) \langle \Psi | \hat{\mathcal{A}} | \Psi \rangle = \overline{\langle \Psi | \hat{\mathcal{A}} | \Psi \rangle} = \sum_{i,j} \overline{c_i c_j^*} \langle \psi_j | \hat{\mathcal{A}} | \psi_i \rangle, \quad (2.10)$$

where \mathcal{P}_k is the statistical weight of $|\Psi\rangle$ in an ensemble of k systems. A density matrix $\hat{\sigma}$ can then be defined as

$$\hat{\sigma} = \sum_k \mathcal{P}_k(\Psi) |\Psi\rangle \langle \Psi| = \sum_k \mathcal{P}_k(\Psi) c_i c_j^* |\psi_i\rangle \langle \psi_j| \quad (2.11)$$

with elements

$$\hat{\sigma}_{ij} = \langle \psi_j | \hat{\sigma} | \psi_i \rangle = \overline{c_i c_j^*}. \quad (2.12)$$

Since the diagonal elements $\hat{\sigma}_{ii}$ of the $2^N \times 2^N$ density matrix of a spin- $\frac{1}{2}$ ensemble have the form $\overline{|c_i|^2}$, they correspond to the populations of the eigenstates $|\psi_i\rangle$ and are real, positive numbers given by the Boltzmann distribution. The off-diagonal elements $\hat{\sigma}_{ij}$ are a measure of the phase coherence belonging to zero-, single- and multiple-quantum transitions ($\Delta m_I = \pm 0, 1, 2, \dots, N$) between the eigenstates $|\psi_i\rangle$ and $|\psi_j\rangle$. In thermal equilibrium, however, the members of the different subensembles described by $\mathcal{P}_k(\Psi)$ are uncorrelated, and hence all off-diagonal density matrix elements zero. Neglecting interactions leading to relaxation, the time-evolution of the density matrix can be derived from (2.8) and is described by the Liouville-von Neumann equation:

$$\frac{d}{dt} \hat{\sigma}(t) = -i \left[\hat{\mathcal{H}}, \hat{\sigma}(t) \right] = -i \left(\hat{\mathcal{H}} \cdot \hat{\sigma}(t) - \hat{\sigma}(t) \cdot \hat{\mathcal{H}} \right), \quad (2.13)$$

where $\hat{\mathcal{H}}$ is the time-independent Hamilton operator describing the spin interactions. The formal solution of (2.13) is a “sandwich” expression of the form

$$\begin{aligned} \hat{\sigma}(t = \tau_1 + \tau_2) &= \exp(-i\hat{\mathcal{H}}_2\tau_2) \exp(-i\hat{\mathcal{H}}_1\tau_1) \hat{\sigma}(0) \exp(i\hat{\mathcal{H}}_1\tau_1) \exp(i\hat{\mathcal{H}}_2\tau_2) \\ \text{or briefly } \hat{\sigma}(0) &\xrightarrow{\hat{\mathcal{H}}_1\tau_1} \hat{\sigma}(\tau_1) \xrightarrow{\hat{\mathcal{H}}_2\tau_2} \hat{\sigma}(t) \end{aligned} \quad (2.14)$$

The exponential operators $\hat{\mathcal{H}}_1$ and $\hat{\mathcal{H}}_2$ (propagators) in (2.14) act as rotation operators in an operator subspace spanned by the propagators, the operator present in the density matrix and their commutator. Using (2.14) one can hence calculate the signals observed in an NMR experiment following a sequence of radio-frequency pulses and delays by subsequent application of different time-independent Hamiltonians $\hat{\mathcal{H}}$ to the density matrix.

2.2.1 Product operators

To follow explicitly the evolution of the spin operators during an NMR experiment it is convenient to express the density matrix as a linear combination of orthogonal operators as was done for the state vector in (2.9) (Ernst *et al.*, 1987)

$$\hat{\sigma}(t) = \sum_{i=1}^{4^N} b_i(t) \hat{B}_i \quad \text{with} \quad \hat{B}_i = 2^{(q-1)} \prod_{l=1}^N \left(\hat{C}_{l,u} \right)^{a_{sl}} \quad (2.15)$$

where \hat{B}_i are the so-called product operators, N is the number of spin- $\frac{1}{2}$ nuclei in the spin system, l is the index of the nuclear spin type (say $\hat{C}_1 = I$ or $\hat{C}_2 = S$), u is the axis of the cartesian spin operators (*i.e.* x , y or z), q is the number of one-spin operators (*i.e.* I_u or S_u) in the product and a_{sl} is one, if it equals the number of nuclei in the product (*i.e.* q) and zero for the remaining $N - q$ nuclei. Hence, a two spin- $\frac{1}{2}$ system comprising spins I and S involves ($4^2 =$)16 product operators: the identity operator $\frac{1}{2}\hat{E}$ ($q = 0$), the one-spin operators I_x, I_y, I_z and S_x, S_y, S_z ($q = 1$) and the two-spin coupling operators $2I_zS_z, 2I_zS_y, 2I_zS_x, 2I_yS_z, 2I_yS_y, 2I_yS_x, 2I_xS_z, 2I_xS_y, 2I_xS_x$ ($q = 2$). The advantage of this formalism is that any product operator can be related to the corresponding component of the magnetic moment $\vec{\mu}$ by multiplication with $\gamma\hbar$ and hence ultimately to the net magnetisation.

If the product operators, which are contained in the propagators, in the initial and in the final density matrix (say \hat{C}_x, \hat{C}_y and \hat{C}_z), satisfy the cyclic commutation relationship $[\hat{C}_x, \hat{C}_y] = i\hat{C}_z$, (2.14) simplifies to

$$\hat{C}(t) = e^{-i\hat{C}_x\theta} \cdot \hat{C}_y \cdot e^{i\hat{C}_x\theta} = \hat{C}_y \cos \theta - i [\hat{C}_x, \hat{C}_y] \sin \theta = \hat{C}_y \cos \theta + \hat{C}_z \sin \theta \quad (2.16)$$

which is a rotation of \hat{C}_y about the \hat{C}_x -axis in the operator space spanned by \hat{C}_x, \hat{C}_y and \hat{C}_z .

2.2.2 Spin interaction Hamiltonians

According to (2.13) and (2.14) the initial product operator, the product operator contained in the interaction Hamiltonian and their commutator need to be known to describe an NMR experiment. Since the dominating interaction in NMR is the interaction with the static magnetic field (high-field approximation), to first order only those interactions have to be considered, which commute with the Zeeman Hamiltonian (secular terms). Spin Hamiltonians have the general form

$$\hat{\mathcal{H}} = c \cdot \vec{I} \vec{T} \vec{S}, \quad (2.17)$$

where c is a constant specific to the interaction of interest. \vec{I} represents a spin vector and \vec{S} either a spin vector or an external magnetic field. In the latter case, \vec{S} is the static field of the superconducting magnet or the oscillating weak field of the RF-pulse. For internal spin

interaction, which refer to intra- and/or intermolecular interactions, \vec{S} is a spin vector (except for the chemical shift where \vec{S} is \vec{B}_0), while the second-rank tensor \tilde{T} contains the orientational dependence of the interaction between the two vectors \vec{I} and \vec{S} . The frame, in which \tilde{T} is diagonal, is referred to as principal axis system (PAS) with the principal elements T_{XX} , T_{YY} and T_{ZZ} ($|T_{ZZ}| \geq |T_{YY}| \geq |T_{XX}|$). The polar angles θ and ϕ describe then the orientation of the PAS of the interaction tensor with respect to the laboratory frame (*e.g.* the direction of the static magnetic field). The average of the tensor trace $\tilde{T}_{iso} = \frac{1}{3}\text{Tr}\{\tilde{T}\} = \frac{1}{3}(T_{XX} + T_{YY} + T_{ZZ})$ determines the observable value for the interaction in isotropic solution. The anisotropy and asymmetry of the tensor are defined as $\delta = T_{ZZ} - T_{iso}$ and $\eta = (T_{YY} - T_{XX})/T_{ZZ}$, respectively. The latter can assume values between one (for fully asymmetric tensors) and zero (for axially symmetric tensors).

In the high-field approximation only terms parallel to B_0 conserve the Zeeman energy. Hence only T_{zz} has to be considered, which is then given by

$$T_{zz}(\phi, \theta) = T_{iso} + \frac{1}{2}\delta (3 \cos^2 \theta - 1 + \eta \sin^2 \theta \cos 2\phi) \quad (2.18)$$

2.2.3 External spin interactions

Zeeman interaction

The energies of the nuclear spin energy levels in an external, static magnetic field can be derived from the classical potential of a dipole in an applied field

$$E = -\vec{\mu} \times \vec{B}_0. \quad (2.19)$$

If the external field is defined along the z -axis, the Zeeman Hamiltonian responsible for the precession of the spins is given by

$$\hat{\mathcal{H}}_Z = -\mu_z \cdot B_0 = -\gamma I_z B_0 = -\omega_0 I_z. \quad (2.20)$$

Irradiation by a radio-frequency pulse

During a radio-frequency pulse, the spin system interacts with the circularly polarised magnetic field of the RF-pulse B_1 , which rotates in the x, y -plane at or close to the Larmor frequency. If the pulse is applied along the x -axis, the Hamiltonian describing the interaction is

$$\begin{aligned} \hat{\mathcal{H}}_{RF} &= -\gamma \hbar B_1 [I_x \cos(\omega_{RF}t) + I_y \sin(\omega_{RF}t)] \\ &= \omega_1 \hbar [I_x \cos(\omega_{RF}t) + I_y \sin(\omega_{RF}t)]. \end{aligned} \quad (2.21)$$

The time-dependence in (2.21) can be removed by transforming the static coordinate system (referred to as laboratory frame) into a coordinate system rotating at Larmor frequency (rotating frame). In the rotating frame, the detector (or the observer) is rotating at the same frequency as the circularly polarised field that matches the Larmor frequency. The RF-field then appears to be static and the Hamiltonian simplifies to

$$\hat{\mathcal{H}}'_{RF} = \omega_1 I_x, \quad (2.22)$$

where $\hat{\mathcal{H}}'_{RF}$ is the Hamiltonian describing the interaction between the spin system and an x -pulse in the rotating frame.

2.2.4 Internal spin interactions

All internal spin interaction Hamiltonians consist of secular and non-secular terms. The latter indicate that spin transitions are induced, which do not conserve the Zeeman energy of the spins and are therefore only relevant for relaxation in the high-field limit. Consequently, for the evolution of the spin coherences only the energy conserving secular terms are considered.

Chemical shift

The chemical shift arises from the interaction of a nuclear spin I with the induced local magnetic field generated by the electrons surrounding the nucleus. The chemical shift Hamiltonian is given by

$$\hat{\mathcal{H}}_{CS} = \gamma_I \vec{I} \cdot \vec{\sigma} \cdot \vec{B}_0 = \gamma_I I_z \sigma_{zz} B_0, \quad (2.23)$$

where $\vec{\sigma}$ is the shielding tensor. Considering only the secular part of the interaction (*i.e.* the part that commutes with I_z), only the shielding in the same direction as the magnetic field has to be taken into account. The PAS, however, can have any orientation with respect to the applied field and therefore σ_{zz} is a combination of the principle values of the chemical shift tensor

$$\sigma_{zz} = \sigma_{iso} + \sigma_{ZZ} \cdot \frac{1}{2} [(3 \cos^2 \theta - 1) + \eta \sin^2 \theta \cdot \cos 2\phi]. \quad (2.24)$$

In isotropic solution the molecules undergo fast random motions and the angular dependence of the interaction vanishes. As a consequence, the shielding tensor reduces to its isotropic value σ_{iso} , which is equivalent to σ_i used in (2.5). However, due the rotational reorientation of the molecules in isotropic solution, the local magnetic field fluctuates randomly at the site of the nucleus. The chemical shift anisotropy (CSA) is therefore a source of relaxation.

Scalar coupling

For the indirect dipole-dipole interaction mediated via bond electrons between the interacting

nuclei, the Hamiltonian is given by

$$\hat{\mathcal{H}}_J = 2\pi \vec{I} \tilde{J} \vec{S} = 2\pi J_{I,S} \left[2I_z S_z + \frac{1}{2}(I^+ S^- + I^- S^+) \right] = 2\pi J_{I,S} 2I_z S_z. \quad (2.25)$$

In the weak coupling limit ($J_{I,S} \ll |\omega_I - \omega_S|$) the flip-flop terms ($I^+ S^-$ and $I^- S^+$) vanish, such that the right most equality in (2.25) remains. The scalar coupling constant measured in isotropic solution is given by $J = \frac{1}{3} \text{Tr}\{\tilde{J}\}$. Since only in-phase ($I_{x,y}$ and $S_{x,y}$) and anti-phase ($2I_{x,y} S_z$ and $2I_z S_{x,y}$) coherences permute in a cyclic manner with $2I_z S_z$, only these coherences evolve scalar coupling during a period of free precession (delay), which allows to transfer magnetisation from spin I to spin S and *vice versa* by J -coupling.

Direct dipolar coupling

In contrast to the *indirect* dipolar coupling interaction, the magnetic field of a spin I can directly interact with the magnetic field of another spin S . The Hamiltonian of the direct dipole-dipole interaction has the form

$$\hat{\mathcal{H}}_D = \frac{c_{I,S}}{r^3} \vec{I} \tilde{D} \vec{S} = \frac{c_{I,S}}{r^3} \cdot \frac{1}{2}(3 \cos^2 \theta - 1) \left[2I_z S_z + \frac{1}{2}(I^+ S^- + I^- S^+) \right], \quad (2.26)$$

where $c_{I,S} = \frac{\mu_0}{4\pi} \gamma_I \gamma_S$ is the dipolar interaction constant and θ the angle between the internuclear vector and the direction of the static magnetic field. The flip-flop terms ($I^+ S^-$ and $I^- S^+$) vanish in the weak coupling limit ($c_{I,S} \ll |\omega_I - \omega_S|$), which is always valid in the case of heteronuclear dipolar coupling. The secular part of the Hamiltonian is hence given by

$$\hat{\mathcal{H}}_D = \frac{c_{I,S}}{r^3} \cdot \frac{1}{2}(3 \cos^2 \theta - 1) 2I_z S_z. \quad (2.27)$$

As \tilde{D} is a traceless tensor, the direct dipolar interaction is not observable in isotropic solution. However, in anisotropic solutions or due to the intrinsic magnetic susceptibility of the biomolecule a certain residual orientation of the dipole-dipole vector remains giving rise to a residual dipolar coupling constant (RDC) (Tolman *et al.*, 1995; Tjandra & Bax, 1997). The RDCs measured for a molecular entity can be described in terms of an alignment tensor, which allows to determine the average orientation of the internuclear vectors with respect to the alignment frame and hence to each other, yielding *a priori* long-range information for the structure refinement (Tjandra *et al.*, 1997b; Clore *et al.*, 1998).

Moreover, the direct dipole-dipole interaction is the source of proton-proton distance restraints, as the nuclear Overhauser effect (NOE) arises from the distance dependent magnetisation transfer by cross-relaxation effects between two magnetic dipoles.

2.2.5 Multi-dimensional NMR

NMR spectroscopy deals with two major problems limiting the size of amenable biomolecules to currently 50 kDa. On the one hand, the low sensitivity of the method leads to poor signal-to-noise ratios, while on the other hand spectral overlap increases considerably with molecular weight. Therefore, spectra are recorded at high magnetic field strengths (currently 500–800 MHz proton frequency) and biomolecules are nowadays labelled routinely with ^{13}C and/or ^{15}N (see Section 3.2). This allows to record heteronuclear multi-dimensional spectra, in which each peak is labelled by up to three different frequencies (^1H , ^{15}N and ^{13}C chemical shifts) and the spectral resolution is hence increased considerably. However, a complete description of the spin system's evolution using the density matrix formalism becomes quickly cumbersome. Instead one can use the so-called product operator formalism (Packer & Wright, 1983; Sørensen *et al.*, 1983; van de Ven & Hilbers, 1983), which describes the evolution of weakly coupled spin- $\frac{1}{2}$ systems in a classical and hence fairly straightforward way. The density operator $\hat{\sigma}$ is represented by the product operators, which can be easily related to the observable magnetisation. The three main interactions during an NMR experiment, radio-frequency pulses, free precession and scalar coupling, are expressed as simple rotations of the product operators in the sub-spaces spanned by the involved operators. All possible rotations leading to a change of the spin state can then conveniently be described by a branch diagram (van de Ven, 1995)

$$C_q \xrightarrow{C_p(\theta)} \begin{cases} C_q \cos \theta \\ -i[C_p, C_q] \sin \theta, \end{cases} \quad (2.28)$$

where C_q denotes the product operator related to the initial density matrix (*e.g.* I_z , if the system is in thermal equilibrium), C_p is the product operator included in the interaction Hamiltonian as defined in subsections 2.2.3 and 2.2.4, while θ is defined differently for each spin interaction.

Chemical shift evolution: Free precession is described as a rotation about the direction of the static magnetic field. Consequently, θ is the product of the spin's Larmor frequency and the time, for which the chemical shift evolves ($\Omega_{I,S}t$). C_p is the longitudinal one-spin operator of the evolving spin (I_z or S_z) as given by (2.23). For instance, in-phase x -magnetisation of spin I evolves as

$$I_x \xrightarrow{I_z \Omega_I t} \begin{cases} I_x \cos(\Omega_I t) \\ -i[I_z, I_x] \sin(\Omega_I t) = I_y \sin(\Omega_I t) \end{cases}$$

J -coupling: J -coupling is described as a rotation about the two-spin axis $2I_z S_z$ (see (2.25)).

Hence, θ includes the product of the coupling constant J and the time τ , for which the

scalar coupling is “active” ($\pi J_{I,S}\tau$). Setting for example τ to $1/(2J_{I,S})$ yields

$$I_x \xrightarrow{2I_z S_z \pi J_{I,S} \tau} \begin{cases} I_x \cos(\pi J_{I,S} \cdot 1/2J_{I,S}) = I_x \cos(\frac{\pi}{2}) = 0 \\ -i[2I_z S_z, I_x] \sin(\pi J_{I,S} \cdot 1/2J_{I,S}) = 2I_y S_z \sin(\frac{\pi}{2}) = 2I_y S_z \end{cases}$$

RF-pulses: The effect of an RF-pulse is described as precession about the direction of the RF-pulse. Since the magnetic field of the RF-pulse is weak compared to the static magnetic field, θ is simply the flip angle β of the RF-pulse and C_p the axis, along which the pulse is applied (see (2.21)). A 90° -pulse applied along the $-y$ -axis on in-phase x -magnetisation of spin I yields z -magnetisation

$$I_x \xrightarrow{-I_y \beta} \begin{cases} I_x \cos(\beta) = I_x \cos(\frac{\pi}{2}) = 0 \\ -i[-I_y, I_x] \sin(\beta) = I_z \sin(\frac{\pi}{2}) = I_z \end{cases}$$

Hence delays and pulses can be applied such that the magnetisation is transferred to the desired coherences in a well-determined way. If each product operator involved in the interaction commutes with the others, the evolution period can be divided into a series of independent rotations, for instance for chemical shift evolution and scalar coupling ($[I_z, 2I_z S_z] = 0$) or selective pulses ($[I_x, S_x] = 0$), which further simplifies the description of pulse sequences. The most important experiments used for structure determination are described in detail in a recent review (Sattler *et al.*, 1999).

All multi-dimensional NMR experiments can be broken down into four major building blocks (Ernst *et al.*, 1987): (i) a preparation period, during which a coherent non-equilibrium state is generated. This can involve the creation of transverse magnetisation by a single RF-pulse or the transfer of magnetisation from protons to a less sensitive heteronucleus using one- or two-bond J -couplings. (ii) an evolution period t_1 , during which the prepared coherences evolve and which determines the frequencies in the first dimension (ω_1 -domain). To sample the t_1 -evolution a series of experiments must be carried out with systematic incrementation of t_1 . (iii) a mixing period, during which coherence is transferred from one spin to another either by through-bond interactions (COSY and TOCSY-type experiments) (Aue *et al.*, 1976; Braunschweiler & Ernst, 1983) or through-space (NOESY experiments) (Macura & Ernst, 1980) establishing the correlation between the recorded dimensions. By introducing additional evolution and mixing periods the dimensionality of the experiment can be increased (Griesinger *et al.*, 1987; Oschkinat *et al.*, 1987). (iv) a detection period, during which the transverse magnetisation is recorded that was prepared in the mixing time. Figure 2.2 summarises the most important building blocks of the periods discussed above.

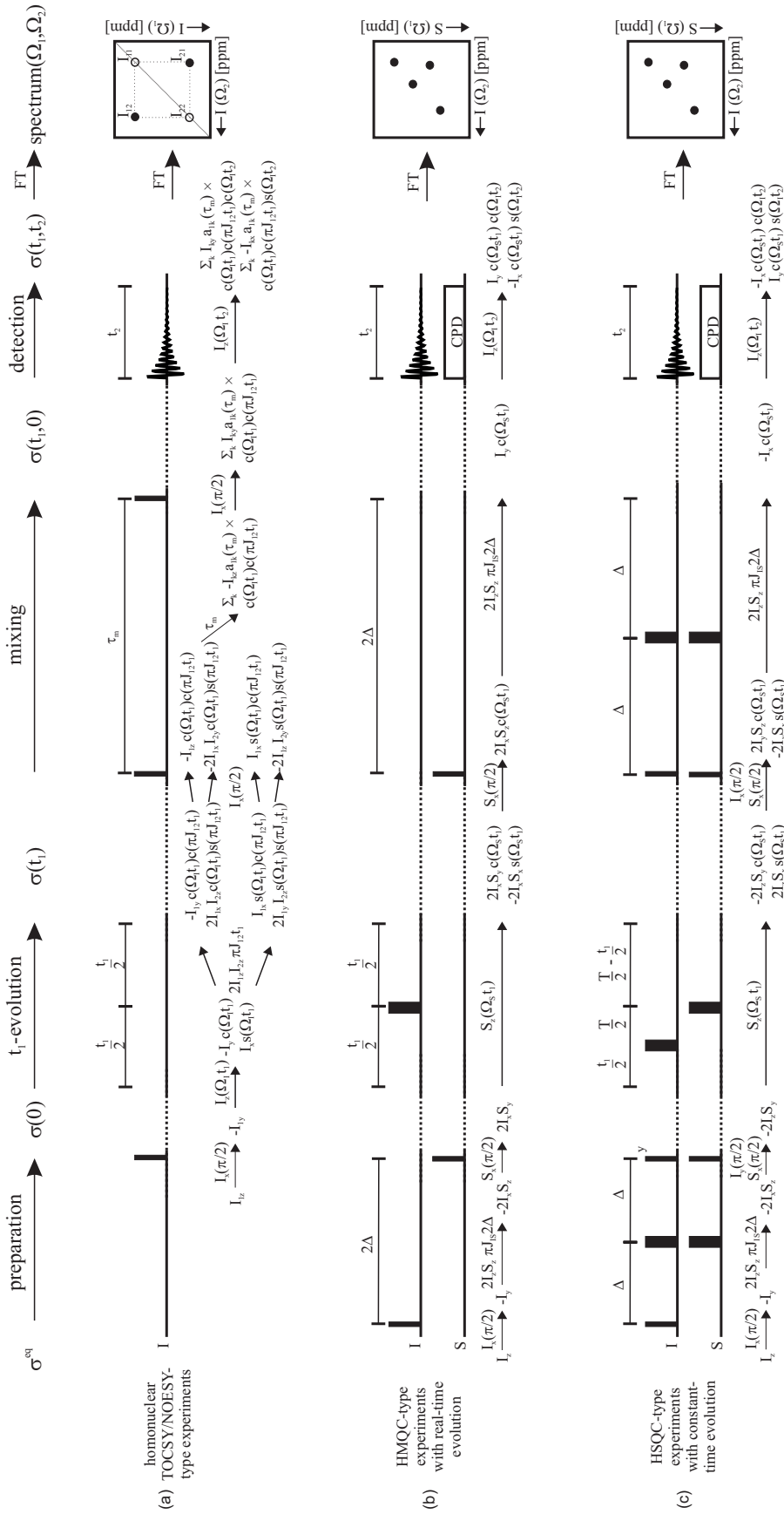


Figure 2.2: Building blocks of multi-dimensional NMR experiments. Top: evolution of the density matrix σ . (a) Homonuclear TOCSY and NOESY experiments (Braunschweiler & Ernst, 1983; Macura & Ernst, 1980). For NOESY experiments, the mixing time τ_m is a pure time delay to transfer magnetisation by dipolar cross-relaxation (*through-space*), while for TOCSY experiments a train of 180° pulses (spin-lock) is applied to transfer magnetisation by J -coupling (*through-bond*). Leaving out the last 90° pulse and τ_m , the pulse sequence corresponds to a COSY experiment (Aue *et al.*, 1976). (b) Heteronuclear multiple-quantum coherence (HMQC) experiments (Müller, 1979) with real time evolution and (c) heteronuclear single-quantum coherence (HSQC) experiments (Bodenhausen & Ruben, 1980) with constant-time evolution. Thin bars denote 90° ($\pi/2$) pulses, while thick bars denote 180° (π) pulses applied along the x -axis, unless specified otherwise. Cosine and sine terms are abbreviated by c and s , respectively. t_1 and t_2 denote the evolution times in the first (indirect) and second (direct) dimension. $\Delta = 1/(4J_{1,2})$ and $T = 1/J_{S_1, S_2}$. Phase cycling and pulsed field gradients have been omitted for reasons of clarity.

2.3 NMR structure determination

Protein structure determination by NMR spectroscopy involves in general the following steps, which are described in more detail in section 3.3: sample preparation, data acquisition, resonance assignment, derivation of structural restraints and structure calculation and validation.

Structure determination by NMR spectroscopy is in general performed on an aqueous solution of the macromolecule(s) of interest. The key to structural information are the chemical shifts, which depend on the electronic environments of the nuclei and hence the identities and distances of nearby atoms. For proteins, protons are the only nuclei with sufficient natural abundance and gyromagnetic ratio to be observed by NMR. However, NMR spectra correlating intra- and interresidual protons suffer severely from spectral overlap with increasing protein sizes. Therefore, proteins with molecular weights above 5 kDa are isotopically enriched with ^{13}C and ^{15}N by overexpression in labelled media. In order to acquire all spectra necessary for structure determination in an adequate time frame the protein must be soluble at high concentration (0.5–1 mM, 5–30 mg/ml) and stable for days without aggregation under experimental conditions.

The suite of multi-dimensional NMR experiments recorded allows to attribute an atom-pair or -triple to each peak in the two- or three-dimensional spectra (resonance assignment). The ultimate result of the spectral analysis is a set of estimates of internuclear distances and angles, called "restraints". The most important restraints in NMR are derived from (a) NOE cross-peak assignment yielding proton-proton distances up to 5 Å (through-space restraints), (b) from 3J -coupling constants giving dihedral angle restraints (through-bond restraints) and (c) from residual dipolar coupling constants and/or local rotational correlation times (in the case of anisotropic tumbling) providing distance-independent projection angle restraints.

Applying the experimental restraints together with geometric and non-bonded parameters known from small molecules in the structure calculation, an ensemble of protein conformations is obtained rather than a single structure. All structures within the ensemble fulfil the structural restraints, representing the NMR solution structure. Comparisons between the structures in the ensemble provides information on how well the protein conformation was determined by the NMR restraints. The r.m.s. (root mean square) deviation between these structures is used to assess how well the structure calculations have converged. Backbone and side-chain dihedral angles are validated by their agreement with the most favoured ϕ, ψ angle combinations (Ramachandran plot) and the clustering of χ_1 -angles at staggered rotamer positions. Regions with a large spread between ensemble structures (often observed in loops or at termini) may result from an insufficient number of restraints, which is often due to internal dynamics of the molecule in solution. The structural quality of an NMR structure is usually summarised in a structural statistics table as provided in Chapter 5 and 7.

As the last step, the obtained structure can be compared with already known structures to identify similar or novel folds. Hydrophobic, hydrophilic and charged clusters as well as cavities within the structure can provide clues to protein stability and interaction potential.

And finally, the importance of residues, such as exposed localisation signals or residues in ligand binding sites, and the consequences of their mutation can be analysed based on the obtained three-dimensional protein structure.

2.4 References

- Abragam, A. (1961). *Principles of nuclear magnetism*. Clarendon Press, Oxford, U.K.
- Aue, W. P., Bartholdi, E. & Ernst, R. R. (1976). Two dimensional spectroscopy: application to nuclear magnetic resonance. *J. Chem. Phys.* **64**, 2229–46.
- Bodenhausen, G. & Ruben, D. J. (1980). Natural abundance nitrogen-15 NMR by enhanced heteronuclear spectroscopy. *Chem. Phys. Lett.* **69**, 185–9.
- Braunschweiler, L. & Ernst, R. R. (1983). Coherence transfer by isotropic mixing: application to proton correlation spectroscopy. *J. Magn. Res.* **53**, 521–8.
- Cavanagh, J., Fairbrother, W. J., Palmer III, A. G. & Skelton, N. J. (1996). *Protein NMR spectroscopy: Principles and Practice*. Academic Press, San Diego, CA.
- Clore, G. M., Gronenborn, A. M. & Tjandra, N. (1998). Direct refinement against residual dipolar couplings in the presence of rhombicity of unknown magnitude. *J. Magn. Res.* **131**, 159–162.
- Ernst, R. R. & Anderson, W. A. (1966). Application of Fourier Transform Spectroscopy to Magnetic Resonance. *Rev. Sci. Instrum.* **37**, 93.
- Ernst, R. R., Bodenhausen, G. & Wokaun, A. (1987). *Principles of nuclear magnetic resonance in one and two dimensions*. Oxford University Press, New York, USA.
- Goldman, M. (1988). *Quantum description of high-resolution NMR in liquids*. Oxford University Press, Oxford, U.K.
- Griesinger, C., Sørensen, O. W. & Ernst, R. R. (1987). A practical approach to three-dimensional NMR spectroscopy. *J. Magn. Res.* **73**, 574–79.
- Jeener, M. (1971). Unpublished lecture at the *Ampère International Summer School II* in Basko polje, Yugoslavia. , .
- Karplus, M. (1963). Vicinal proton coupling in nuclear magnetic resonance. *J. Am. Chem. Soc.* **85**, 2870–1.
- Macura, S. & Ernst, R. R. (1980). Elucidation of cross relaxation in liquids by two-dimensional N.M.R. spectroscopy. *Mol. Phys.* **41**, 95–117.
- Müller, L. (1979). Sensitivity enhanced detection of weak nuclei using heteronuclear multiple quantum coherence. *J. Am. Chem. Soc.* **101**, 4481–4.
- Oschkinat, H., Griesinger, C., Kraulis, P., Sørensen, O. W., Ernst, R. R., Gronenborn, A. M. & Clore, G. M. (1987). Three-dimensional NMR spectroscopy of a protein in solution. *Nature*, **332**, 374–376.

- Packer, K. J. & Wright, K. M. (1983). The use of single-spin operator basis-sets in the NMR spectroscopy of scalar coupled spin systems. *Mol. Phys.* **50**, 797–813.
- Pervushin, K., Riek, R., Wider, G. & Wüthrich, K. (1997). Attenuated T2 relaxation by mutual cancellation of dipole-dipole coupling and chemical shift anisotropy indicates an avenue to NMR structures of very large biological macromolecules in solution. *Proc. Natl. Acad. Sci. USA*, **94** (23), 12366–71.
- Sattler, M., Schleucher, J. & Griesinger, C. (1999). Heteronuclear multidimensional NMR experiments for the structure determination of proteins in solution employing pulsed field gradients. *Prog. NMR Spectrosc.* **34**, 93–158.
- Sørensen, O. W., Eich, G. W., Levitt, M. H., Bodenhausen, G. & Ernst, R. R. (1983). Product operator formalism for the description of NMR pulse experiments. *Prog. NMR Spectrosc.* **16**, 163–192.
- Tjandra, N. & Bax, A. (1997). Direct measurement of distances and angles in biomolecules by NMR in a dilute liquid crystalline medium. *Science*, **278**, 1111–1114.
- Tjandra, N., Garrett, D. S., Gronenborn, A. M., Bax, A. & Clore, G. M. (1997a). Defining long range order in NMR structure determination from the dependence of heteronuclear relaxation times on rotational diffusion anisotropy. *Nat. Struct. Biol.* **4**, 443–9.
- Tjandra, N., Omichinski, J. G., Gronenborn, A. M., Clore, G. M. & Bax, A. (1997b). Use of dipolar ^1H - ^{15}N and ^1H - ^{13}C couplings in the structure determination of magnetically oriented macromolecules in solution. *Nat. Struct. Biol.* **4**, 732–738.
- Tolman, J. R., Flanagan, J. M., Kennedy, M. A. & Prestegard, J. H. (1995). Nuclear magnetic dipole interactions in field-oriented proteins: information for structure determination in solution. *Proc. Natl. Acad. Sci. USA*, **92**, 9279.
- van de Ven, F. J. M. (1995). *Multidimensional NMR in liquids*. VCH Publishers, Inc., New York, USA.
- van de Ven, F. J. M. & Hilbers, C. W. (1983). A simple formalism for the description of multiple-pulse experiments. Application to a weakly coupled two-spin ($I=1/2$) system. *J. Magn. Res.* **54**, 512–20.